Measurement of the conductance of single conjugated molecules

Tali Dadosh[1,2]*, Yoav Gordin[1]*, Roman Krahne[1]†, Ilya Khivrich[1], Diana Mahalu[1], Veronica Frydman[3], Joseph Sperling[2], Amir Yacoby[1] & Israel Bar-Joseph[1]

Electrical conduction through molecules depends critically on the delocalization of the molecular electronic orbitals and their connection to the metallic contacts. Thiolated (−SH) conjugated organic molecules are therefore considered good candidates for molecular conductors[1,2]: in such molecules, the orbitals are delocalized throughout the molecular backbone, with substantial weight on the sulphur–metal bonds[1–4]. However, their relatively small size, typically ∼1 nm, calls for innovative approaches to realize a functioning single-molecule device[5–11]. Here we report an approach for contacting a single molecule, and use it to study the effect of localizing groups within a conjugated molecule on the electrical conduction. Our method is based on synthesizing a dimer structure, consisting of two colloidal gold particles connected by a dithiolated short organic molecule[12,13], and electrostatically trapping it between two metal electrodes. We study the electrical conduction through three short organic molecules: 4,4′-biphenyldithiol (BPD), a fully conjugated molecule; bis-(4-mercaptophenyl)-ether (BPE)[14], in which the conjugation is broken at the centre by an oxygen atom; and 1,4-benzenedimethanethiol (BDMT), in which the conjugation is broken near the contacts by a methylene group. We find that the oxygen in BPE and the methylene groups in BDMT both suppress the electrical conduction relative to that in BPD.

Various methods have been suggested and realized to form nanometre-sized gaps, including electron beam lithography with shadow mask evaporation[15], mechanical break junctions[5–7], electromigration[8], and side etched quantum wells[16]. Molecules are then deposited on the thin gap, and it is assumed that electrical conductivity is obtained when a single molecule bridges the gap and conducts current. Although impressive success in measuring the conductance of molecular junctions has been reported[5–7,9,10,17], serious problems are evident. The most notable are the uncertainty about the number of conducting molecules in the junction, and the lack of information about the shape and structure of the metal contacts near the molecule. The dimer-based contacting scheme presented here provides several advantages. (1) Single-molecule devices can be fabricated with high certainty. (2) The contacts to the molecule are well defined and can be characterized separately. (3) Our scheme avoids the need for fabricating nanometre-sized gaps. (4) It also allows measurements of the temperature dependence of the molecular junction conductance over periods of hours and even days, regaining the original spectra after thermal cycling.

The dimer synthesis is performed by mixing a solution of dithiolated molecules, whose structure is depicted in Fig. 1a, with a gold colloid, keeping their respective ratio below 1:10. The colloids were stabilized using the conventional citrate method[18]. In making the bridged dimers, the thiols on the bridging molecule displace citrate

anions to form stable Au–S bonds[19] (Fig. 1b, c). If more than one molecule binds to a certain colloidal particle, trimers (Fig. 1d), tetramers (Fig. 1e) and higher oligomers can be formed. To ensure that most of the dimeric colloidal particles are bridged by a single dithiolated molecule, the concentration of the latter (C_m) in the reaction mixture should be much smaller than the concentration of the monomeric colloidal particles (C_p). In that case, when the reaction is completed, the ratio R of dimers to single unbound colloidal particles is expected to follow the relation $R \approx C_m/(C_p - 2C_m)$. We measured R for different input concentrations of dithiolated molecules, keeping C_p fixed, and found that the above relation holds for C_m:C_p ratios that are lower than 1:10.

The dimeric colloidal particles are separated from monomeric particles and higher oligomers on the basis of their relative mass, by centrifugation through glycerol or sucrose density gradients. Each structure propagates as a different band along the centrifuged tube, and is easily distinguished because of its reddish colour. Figure 1f shows a transmission electron microscope (TEM) image at higher magnification of a dimer (made of two 10-nm colloidal gold particles connected by BDMT) that was synthesized in this manner. The gap between the two particles is readily seen, and its size is in good agreement with the size of the BDMT molecule, which is
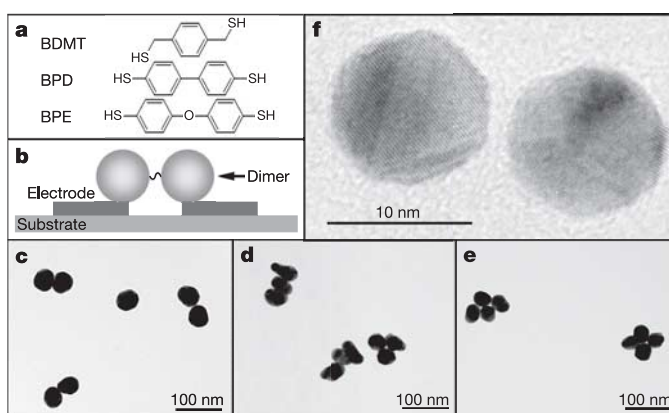

Figure 1 | The molecules and colloidal structures under study. a, The structures of the three molecules: 1,4-benzenedimethanethiol (BDMT), 4,4′-biphenyldithiol (BPD) and bis-(4-mercaptophenyl)-ether (BPE). **b**, The dimer contacting scheme. **c–e**, TEM images of BDMT dimer, trimer and tetramer structures made of 50-nm colloidal gold particles. **f**, TEM image of a BDMT dimer made of 10-nm colloidal gold particles. The ∼1 nm separation between the two particles corresponds approximately to the BDMT length (0.9 nm).

[1]Department of Condensed Matter Physics, [2]Department of Organic Chemistry, [3]Chemical Research Support, Weizmann Institute of Science, 76100 Rehovot, Israel.
†Present address: National Nanotechnology Labs of INFM, Lecce 73100, Italy.
*These authors contributed equally to this work.

approximately 0.9 nm. To further establish the presence of a molecule in the dimer, we conducted Raman scattering measurements on dimers made from colloidal silver particles[20]. A clear Raman spectrum was detected from a single dimer, with the characteristic temporal blinking of a single molecule.

We position the dimer between two electrodes using the method of electrostatic trapping[15,16,21]. The gold electrodes are defined on a silicon substrate with a thin (25–100 nm) oxide layer using electron beam lithography. In most of our studies we use dimers of 30-nm-diameter colloidal gold particles. Hence, the electrodes are made with 40–50 nm separation, which is below the dimer size and larger than the diameter of a single particle. The processed structures are first cleaned[22] and then inserted in a probe station where the electrostatic trapping is performed.

The success rate of the electrostatic trapping is relatively high, and reaches ~50% when the impedance of the dimer solution is high enough, such that the dipole–dipole interaction between the electrodes and the colloids is not screened. An analysis of the trapping events reveals that in 55% of the cases the gap is bridged by one colloidal particle only. In 45% of the cases we get a dimer between the two electrodes (Fig. 2a): in 35% the conductivity is too low to determine the conductance features. We find in scanning electron microscopy (SEM) imaging that the brightness of the colloidal gold particles of these dimers is low, probably due to poor conductivity between one of the particles and the electrode[23]. In 10% of the trapping events we obtain high conductivity dimers. These are the samples that we refer to here: 11 BPD, 13 BPE and 15 BDMT devices.

Trapping single colloidal particles between closely spaced electrodes (25–30 nm) allows us to study the current–voltage characteristics of the contacts. For the 30-nm colloidal gold particles, we find a Coulomb blockade staircase with a single electron charging energy of ~20–30 meV, and by applying a voltage to the substrate we can measure the diamond structure of the conductance (see Supplementary Fig. 1) characteristic of a single-electron transistor[24]. It is evident that a tunnel barrier with a typical resistance of ~10 MΩ is formed between the gold particles and the electrodes, probably due to the ligands that stabilize the colloids in the solution.

The measurements of electrical transport through the dimer structures are performed using an a.c. voltage with an amplitude of a few millivolts superimposed on a d.c. voltage, and the current as well as the differential conductance (dI/dV) are measured
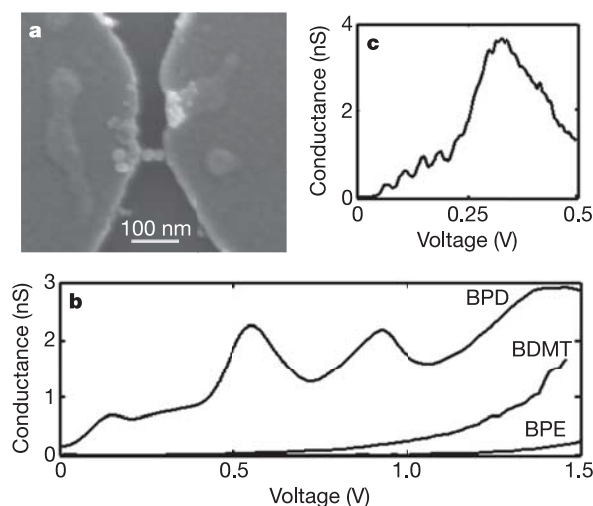

Figure 2 | Image and low-temperature differential conductance spectra of dimers. a, SEM image of a dimer trapped between the two electrodes. **b,** The differential conductance as a function of voltage measured for BPD, BDMT and BPE dimers at 4.2 K. **c,** Coulomb blockade oscillations of the colloidal gold particle which are superimposed on the conduction peak of BPD measured at 4.2 K.
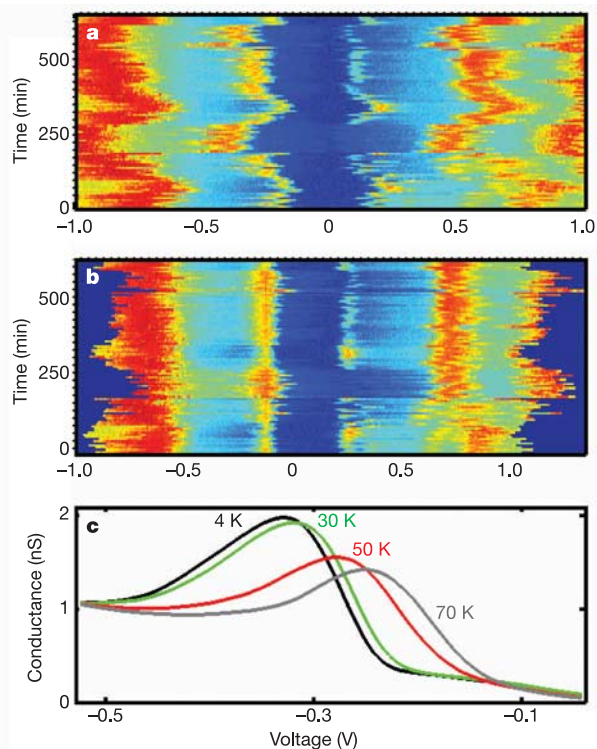

Figure 3 | Temporal fluctuations and temperature dependence of the dimer conductance. a, A compilation of 130 measurements of the differential conductance spectrum of one BPD dimer, taken over a period of a few hours. The conductance values are represented by a colour scale, which ranges from blue (0 nS) to red (3 nS). **b,** The spectra of **a** shifted such that their peaks at −0.2 V coincide, thus demonstrating the rigid shift nature of the temporal fluctuations. **c,** The evolution of the lowest voltage conductance peak of a BPD dimer with temperature. A decrease in height and broadening of the peak with increasing temperature are observed.

simultaneously. Figure 2b shows a comparison of the differential conductance of the three molecules at 4 K. These are representative curves from more than ten devices of each of the molecular species that were studied. The BPD dimers clearly show a series of conductance peaks. These peaks cannot be attributed to charging of the gold particles—their typical spacing is a few hundred millivolts, more than an order of magnitude larger than the charging energy of the particles. In fact, in some cases we could resolve the Coulomb blockade oscillations superimposed on the large conduction peaks (see Fig. 2c). The oscillation period is very similar to that observed in a single-particle measurement (see comparison in Supplementary Information). We note that the conductance through a single trapped colloidal particle is substantially higher than that of a dimer, typically by one to two orders of magnitude. Hence, the tunnel barriers between the metal electrodes and the gold particles act as small series resistances, carrying only a minute fraction of the applied voltage, while most of the voltage is dropped across the molecule.

The BPE and BDMT dimers show remarkably different behaviours. It is clearly seen that the conduction through the dimers formed from these molecules turns on at much higher voltages (typically larger than 0.5 V) and one cannot resolve any peak structure. The systematic difference between the three molecules further confirms that the measured differential conductance is of molecular origin. The apparent gap and exponential turn-on of the differential conductance in the case of the BPE and BDMT dimers suggest that adding localizing groups interferes with the conjugated aromatic system and suppresses the overall conductance through the molecule. This assertion is supported by comparing the BPE with the BPD molecule, where the addition of an oxygen atom between

678

the conjugated rings suppresses the conductance almost entirely below 1 V. A similar effect takes place in the BDMT dimers, where the methylene groups suppress the overlap of the molecular backbone orbitals with the contacts[25].

Focusing on the peak structure of the BPD dimers, we find that while the main features of the conductance spectrum are highly reproducible, there are temporal fluctuations as well as variations between different devices. Figure 3a shows a compilation of 130 measurements of the conductance of one dimer taken over a period of a few hours. Strong temporal fluctuations in peak position, which could be as large as a few hundred millivolts, are evident. We find that the conductance spectrum shifts rigidly—that is, all peaks at positive and negative voltages move in the same direction by approximately the same value. This is demonstrated in Fig. 3b, where we shift all spectra such that their peaks at −0.2 V coincide. It is seen that this operation causes all other peaks to be aligned as well. Such behaviour is typical of electrostatically gated Coulomb blockaded systems with different input and exit capacitances[24]. Plotting the conductance in the V_{ds}–V_g plane (where V_{ds} and V_g are the drain–source and gate voltages, respectively) produces a skewed diamonds structure (see Supplementary Fig. 1b). It can be seen that under these conditions the conductance peaks at positive and negative drain–source bias indeed move rigidly on application of a gate voltage. As the gold particles are very effective in screening the effect of remote potentials, we conclude that charge movement in close vicinity to the molecule gives rise to the observed rigid shift of the spectrum. These temporal fluctuations can therefore be considered as evidence for gating of the molecule, which occurs randomly. We note that the temporal frequency of this random gating depends on the voltage sweep rate, dV/dt, and the voltage range of the measurement. It could be substantially minimized by working at low sweep rates and within a limited voltage range, such that stable and reproducible measurements can be conducted over hours.

The dimer structure allows us to conveniently perform measurements of the temperature dependence of the molecular junction conductance. We demonstrate this capability in Fig. 3c, which shows the behaviour of the lowest voltage peak ($\sim$ −0.3 V in Fig. 3a) as the temperature is increased from 4 K to 100 K. It is evident that the peak broadens and decreases in height with increasing temperature, keeping the area approximately constant. The shift in peak position between the low- and high-temperature measurements is due

to gating, which occurred during this long measurement. The broadening of the peak can be accounted for by the change in thermal distribution of the electrons in the leads. This mechanism is expected to broaden the peak by $\sim 2 k_B T$ (half-width at half-maximum), where k_B is the Boltzmann constant.

Comparing the conductance of nine BPD dimer-based devices shows that the variations between devices in the positions and relative strengths of the peaks cannot be explained only as a rigid shift. This is demonstrated in Fig. 4a, which compares the spectra of two BPD dimers. We can see that while the main features appear at approximately the same voltages, one cannot align the two spectra by a simple shift operation. We note also that there are differences in the value of the conductance between the various devices, which can be as large as an order of magnitude. To statistically quantify this variability, we construct a histogram of peak positions (Fig. 4b). This is done by converting each spectrum to a set of peaks, each represented by a block of unit height, a width which is the full-width at half-maximum, and is centred around its maximum. A rigid shift of each spectrum was allowed to accommodate the temporal fluctuations. It is seen that the peak structure survives the averaging over many molecules, indicating that the variability in peak position is smaller than the peak spacing. The peak positions determined from the histogram agree very well with measurements done on self-assembled monolayers of BPD[26]. However, such agreement is lacking when comparing the measured spectra with recent calculations of molecular conduction[3,4]. In particular, the measured turn-on voltage is significantly lower than theoretically predicted. Moreover, the predicted conductance is several orders of magnitude higher than observed.

METHODS

Colloidal gold nanoparticles with a diameter of 30 nm were prepared using a method described by Grabar et al.[18], with slight modifications. Briefly, a solution of 'seed colloid' (2.6 nm) was prepared by adding 1.0 ml of 10 mg ml^{-1} aqueous HAuCl$_4$·3H$_2$O to 100 ml of Milli-Q water while stirring. One min later, 1.0 ml of 10 mg ml^{-1} aqueous trisodium citrate was added, followed, 1 min later, by 1.0 ml of freshly prepared 0.75 mg ml^{-1} NaBH$_4$ in water, and the mixture was stirred for 5 min. Larger colloidal particles, 30 nm in diameter, were prepared by adding 0.2 ml of 10 mg ml^{-1} trisodium citrate and 130 μl of the Au 'seed colloid' solution to 50 ml of a boiling aqueous solution of HAuCl$_4$·3H$_2$O (0.1 mg ml^{-1}) while stirring. Refluxing was continued for 10 min, or until a change to a reddish colour was observed. This procedure resulted in a citrate-stabilized colloid of gold particles well-dispersed in water[27]; the particles had a narrow size distribution[28], as confirmed by TEM. The concentration of colloidal gold particles was calculated on the basis of mean particle diameter measured by TEM and the weight of HAuCl$_4$ used in the reaction[19].

The dimer preparation consisted of several stages. First, the colloidal gold solution was concentrated. This was achieved by centrifuging the solution at $9.7 \times 10^3 g$ for 5 min and discarding the supernatant. The precipitate was resuspended in 2.5 ml of 1 mM NaOH and centrifuged again as above, leaving about 0.4 ml of concentrated solution. The spacer dithiol molecule was dissolved in 0.1 M NaOH and diluted with 1 mM NaOH to the desired concentration. This solution was mixed with an equal volume of the concentrated colloidal gold solution containing >10-fold molar excess of colloidal particles and incubated for 24 h at 4 °C. The mixture (0.5 ml) was loaded on a 10–75% glycerol gradient in water and centrifuged at $1 \times 10^4 g$ for 10 min in a Beckman SW41 rotor. Fractions (0.5 ml) of the gradient were collected and characterized by TEM.

The electrodes are prepared on an electron beam defined pattern, and consist of 20 nm of Au on 10 nm of Ni that serves as an adhesion layer. The electrodes are cleaned in warm acetone and methanol for 5 min each, then placed in an ozone stripper for 8 min and finally stirred in ethanol for 10 min (ref. 22).

Electrostatic trapping is performed in a probe station; a 0.35 μl drop of the dimer solution (containing typically 45–55% dimers, 40–50% single particles and a few per cent of higher conjugates) is placed on the electrodes' surface. Next an a.c. voltage of 800 mV at 10 MHz is applied between the electrodes for 1 min. The sample is then cleaned in double distilled water, and blown dry in nitrogen. The devices are tested on the probe station, and the ones that show conductivity are bonded and measured at 4 K. After the measurement, the devices are imaged in an SEM to determine the type of colloidal structure that has been trapped.
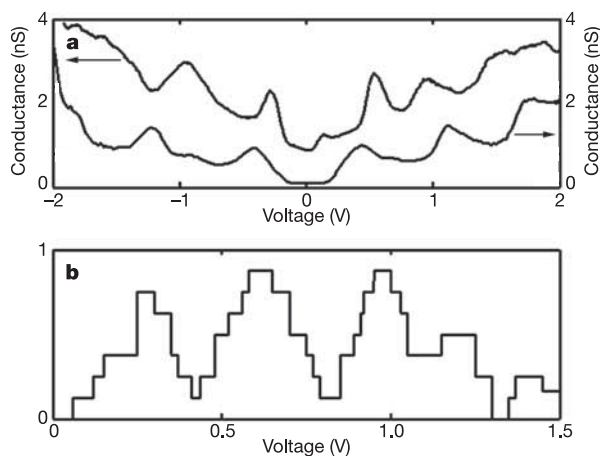

Figure 4 | The reproducibility of the conductance spectra measurements of different BPD dimers. a, Comparison of the differential conductance spectrum of two different BPD devices (the upper curve has been shifted upwards for clarity). **b,** Histogram of the conductance peak positions collected from nine BPD devices. Each spectrum was converted to a set of peaks of unit height and a width which is the full-width at half-maximum. A rigid shift of the spectrum by up to 50 mV was allowed.

Received 20 January; accepted 7 June 2005.

1. Nitzan, A. & Ratner, M. A. Electron transport in molecular wire junctions. *Science* **300**, 1384–1389 (2003).
2. Joachim, C., Gimzewski, J. K. & Aviram, A. Electronics using hybrid-molecular and mono-molecular devices. *Nature* **408**, 541–548 (2000).
3. Xue, Y. & Ratner, M. A. Microscopic study of electrical transport through individual molecules with metallic contacts. I. Band lineup, voltage drop, and high-field transport. *Phys. Rev. B* **68**, 115406–115418 (2003).
4. Remacle, F. & Levine, R. D. Electrical transmission of molecular bridges. *Chem. Phys. Lett.* **383**, 537–543 (2004).
5. Reed, M. A., Zhou, C., Muller, C. J., Burgin, T. P. & Tour, J. M. Conductance of a molecular junction. *Science* **278**, 252–254 (1997).
6. Reichert, J. *et al.* Driving current through single organic molecules. *Phys. Rev. Lett.* **88**, 176804 (2002).
7. Smit, R. H. M. *et al.* Measurement of the conductance of a hydrogen molecule. *Nature* **419**, 906–909 (2002).
8. Park, H., Lim, A. K. L., Alivisatos, A. P., Park, J. & McEuen, P. L. Fabrication of metallic electrodes with nanometer separation by electromigration. *Appl. Phys. Lett.* **75**, 301–303 (1999).
9. Park, J. *et al.* Coulomb blockade and the Kondo effect in single-atom transistors. *Nature* **417**, 722–725 (2002).
10. Liang, W., Shores, M. P., Bockrath, M., Long, J. R. & Park, H. Kondo resonance in a single-molecule transistor. *Nature* **417**, 725–729 (2002).
11. Cui, X. D. *et al.* Reproducible measurement of single-molecule conductivity. *Science* **294**, 571–574 (2001).
12. Peng, X., Wilson, T. E., Alivisatos, A. P. & Schultz, P. G. Synthesis and isolation of a homodimer of cadmium selenide nanocrystals. *Angew. Chem. Int. Edn Engl.* **36**, 145–147 (1997).
13. Brousseau, L. C. III, Novak, J. P., Marinakos, S. M. & Feldheim, D. L. Assembly of phenylacetylene-bridged gold nanocluster dimers and trimers. *Adv. Mater.* **11**, 447–449 (1999).
14. Baron, A. L. & Blank, D. R. Synthesis and properties of some aromatic polythioethers. *Makromol. Chem.* **140**, 83–89 (1970).
15. Bezryadin, A., Dekker, C. & Schmid, G. Electrostatic trapping of single conducting nanoparticles between nanoelectrodes. *Appl. Phys. Lett.* **71**, 1273–1275 (1997).
16. Krahne, R. *et al.* Fabrication of nanoscale gaps in integrated circuits. *Appl. Phys. Lett.* **81**, 730–732 (2002).
17. Park, H. *et al.* Nanomechanical oscillations in a single-C_{60} transistor. *Nature* **407**, 57–60 (2000).
18. Grabar, K. C. *et al.* Two-dimensional arrays of colloidal gold particles: A flexible approach to macroscopic metal surfaces. *Langmuir* **12**, 2353–2361 (1996).
19. Weisbecker, C. S., Merritt, M. V. & Whitesides, G. M. Molecular self-assembly of aliphatic thiols on gold colloids. *Langmuir* **12**, 3763–3772 (1996).
20. Xu, H. X., Bjerneld, E. J., Kall, M. & Borjesson, L. Spectroscopy of single hemoglobin molecules by surface enhanced Raman scattering. *Phys. Rev. Lett.* **83**, 4357–4360 (1999).
21. Amlani, I., Rawlett, A. M., Nagahara, L. A. & Tsui, R. K. An approach to transport measurements of electronic molecules. *Appl. Phys. Lett.* **80**, 2761–2763 (2002).
22. Ron, H., Matlis, S. & Rubinstein, I. Self-assembled monolayers on oxidized metals. 2. Gold surface oxidative pretreatment, monolayer properties, and depression formation. *Langmuir* **14**, 1116–1121 (1998).
23. Hazani, M. *et al.* DNA-mediated self-assembly of carbon nanotube-based electronic devices. *Chem. Phys. Lett.* **391**, 389–392 (2004).
24. Grabert, H. & Devoret, M. H. (eds) *Single Charge Tunneling: Coulomb Blockade Phenomena in Nanostructures* (NATO ASI Ser. B. Vol. 294, Plenum, New York, 1992).
25. Xiao, X. Y., Xu, B. Q. & Tao, N. J. Measurement of single molecule conductance: Benzenedithiol and benzenedimethanethiol. *Nano Lett.* **4**, 267–271 (2004).
26. Lee, J. O. *et al.* Absence of strong gate effects in electrical measurements on phenylene-based conjugated molecules. *Nano Lett.* **3**, 113–117 (2003).
27. Zhu, T., Vasilev, K., Kreiter, M., Mittler, S. & Knoll, W. Surface modification of citrate-reduced colloidal gold nanoparticles with 2-mercaptosuccinic acid. *Langmuir* **19**, 9518–9525 (2003).
28. Handley, D. A. in *Colloidal Gold—Principles, Methods, and Applications* (ed. Hayat, M. A.) 13–32 (Academic, New York, 1989).

CORRIGENDUM

Magnetic carbon

Tatiana L. Makarova, Bertil Sundqvist, Roland Höhne, Pablo Esquinazi, Yakov Kopelevich, Peter Scharff, Valerii A. Davydov, Ludmila S. Kashevarova & Aleksandra V. Rakhmanina

Nature **413**, 716–718 (2001)

In this Letter, there was a mistake in the presentation of the synthesis conditions of the reported samples. The actual range of the temperatures of synthesis for the four rhombohedral samples was 975–1,025 K. One of the five reported samples was wrongly characterized in relation to the polymerization type: the sample was actually prepared at 2.5 GPa (synthesis temperature, 1,125 K), representing a mixture of the rhombohedral and tetragonal phases with some hard carbon. The error in characterization of this sample weakens our attribution of the ferromagnetism to defects in the rhombohedral phase (Rh-C_{60}) but does not influence our main conclusion concerning the observation of magnetism in a carbon solid based on polymerized fullerenes, although its origin and the actual magnitude remain an open question. Also, we were unaware of earlier work on magnetism in polymerized fullerenes[1], that should have been cited.

T.L.M. takes full responsibility for the misidentification of the sample preparation conditions. We thank A. V. Talyzin for alerting us to this mistake.

1. Murakami, Y. & Suematsu, H. Magnetism of C_{60} induced by photo-assisted oxidation. *Pure Appl. Chem.* **68**, 1463–1467 (1996).

CORRIGENDUM

Human contribution to the European heatwave of 2003

P. A. Stott, D. A. Stone & M. R. Allen

Nature **432**, 610–614 (2004)

The description of the method used for the calculation of the fraction attributable risk (FAR) shown in Fig. 4b is incorrect. The corresponding sentence in the Methods section should read "For the red curve, the response to anthropogenic forcing is also included, and a normal distribution is used to estimate the chance of exceeding the 1.6 K threshold."

ERRATUM

Measurement of the conductance of single conjugated molecules

Tali Dadosh, Yoav Gordin, Roman Krahne, Ilya Khivrich, Diana Mahalu, Veronica Frydman, Joseph Sperling, Amir Yacoby & Israel Bar-Joseph

Nature **436**, 677–680 (2005)

In Fig. 4a of this Letter, in which the spectra of two BPD dimmers are compared, the scaling on the two *y* axes should have been shifted relative to one another in order to illustrate the point made in the text. The corrected Fig. 4a is shown here.